

# INTERACTION BETWEEN THE SOLAR WIND AND THE INTERSTELLAR MEDIUM

*Thomas E. Holzer*

High Altitude Observatory, National Center for Atmospheric Research,  
Boulder, Colorado 80307

## 1. INTRODUCTORY REMARKS

Studies of the interaction between the solar wind and the interstellar medium have been carried out with varying degrees of intensity over more than three decades (e.g. early work by Davis 1955, 1962, Parker 1961, 1963, Axford et al. 1963; reviews by Axford 1972, 1973, Fahr 1974, Holzer 1977, Thomas 1978, Lee 1988). The intensity of activity in this field has been determined primarily by the availability of relevant observations, and a recent surge of activity has been generated by the suggestion of a possible indirect detection of the shock transition terminating the supersonic solar wind flow (Kurth et al. 1984, 1987, Lee 1988), by the consequent realization of the possibility that a deep space probe may soon cross this terminal shock, and by recently increased activity in the observational study of the local interstellar medium (e.g. Frisch 1986, Cox & Reynolds 1987). It thus seems an appropriate time for a critical review of the observational and theoretical work on which our current understanding of this subject is based.

The basic dynamical interaction between the solar wind and the interstellar medium involves the relaxation toward pressure equilibrium between the solar and interstellar magnetized plasmas. This interaction leads to the formation of a cavity in the interstellar medium carved out by the solar plasma, which we refer to as the heliospheric cavity, or simply the heliosphere. It is not difficult to determine what heliospheric and interstellar parameters are likely to be important in the interaction between the solar wind and the interstellar medium, and in Section 2 we provide

an overview of the observationally inferred values of these parameters, including the uncertainties in the inferences. Then, in Section 3 we examine from a theoretical point of view the basic physical processes that are likely to be important in this interaction, and we conclude in Section 3.8 by combining this theoretical information with the observational information of Section 2 in an effort to develop the currently most likely overall picture of the heliosphere that is shaped by the local interstellar medium.

## 2. OBSERVATIONAL OVERVIEW

We begin with an overview of currently available observational inferences concerning (a) the relevant properties of the solar wind in its asymptotic flow regime, (b) the nature of the very local interstellar medium (VLISM), and (c) the various modes of interaction between the solar wind and the VLISM. The degree of uncertainty associated with these observational inferences varies greatly, with the inferences concerning the in-ecliptic solar wind being the least uncertain and those concerning the VLISM, particularly the interstellar magnetic field, being the most uncertain. In the present section we simply note the degrees of uncertainty, and in the following sections we discuss the implications of these uncertainties for our understanding of the interaction between the solar wind and the interstellar medium. Some observations that are relevant to the problem at hand are not considered in this section, but these are discussed at an appropriate point in Section 3.

### 2.1 *The Distant Solar Wind*

As noted in Section 1 and discussed in detail in Section 3, the basic dynamical interaction between the solar wind and the VLISM involves the relaxation toward pressure equilibrium between the solar and interstellar magnetized plasmas. The principal solar wind parameter controlling this interaction is the ram pressure of the supersonic flow,  $\rho u^2$ , where  $\rho$  is the mass density, and  $u$  the flow speed of the solar wind. In contrast, the penetration of interstellar hydrogen atoms into the heliosphere and their effects on the solar wind in the regions of supersonic and subsonic flow are largely controlled by the solar wind proton flux density  $n_p u$  (where  $n_p$  is the proton density), the solar wind flow speed  $u$  in the supersonic region, and the solar wind temperature  $T$  in the subsonic region. Thus, the three directly observable solar wind parameters in which we are most interested are  $n_p u$ ,  $u$ , and  $\rho u^2$  in the supersonic solar wind.

The region of supersonic solar wind flow is generally organized (except near the maximum of the 11-yr solar activity cycle) by the dipole component of the solar magnetic field, with relatively low-speed wind flowing

near the dipole equator and relatively high-speed wind flowing at higher magnetic latitudes (e.g. Hundhausen 1977, Hundhausen et al. 1981). Throughout much of the 11-yr cycle (namely, the minimum and post-minimum phases of the cycle) the dipole axis is nearly coincident with the solar rotation axis, but during the declining (postmaximum) phase of the cycle the dipole axis is tilted significantly (some  $30^\circ$ ) with respect to the solar rotation axis. During this latter period the nonalignment of the rotational and magnetic axes gives rise to a strong interaction between high-speed and low-speed solar wind at low and middle solar latitudes (e.g. Hundhausen 1977, Pizzo 1986, Burlaga 1988). Finally, near the maximum of the solar activity cycle, the organizing dipole structure largely disappears, and relatively slow wind flows over most solar latitudes and longitudes (e.g. Sime 1983, Kojima & Kakinuma 1987).

In situ solar wind observations (e.g. Feldman et al. 1977, Schwenn 1983) indicate that the wind parameters of particular interest to us are well organized by solar wind speed, so we should be able to infer reasonable average values for these parameters ( $n_p u$ ,  $u$ , and  $\rho u^2$ ) for all solar latitudes and all phases of the solar activity cycle. (The complicating effects of solar wind stream interactions at low and middle solar latitudes during the declining phase of the solar cycle are discussed in Section 3.) The major uncertainty we confront in determining these values arises from the uncertainty in the absolute measurement of proton density (Feldman et al. 1977). Although the relative accuracy of density measurements by a given instrument is quite good, the absolute (systematic) error may be more than 30% (Feldman et al. 1977), as is evidenced by the intercalibration of the HELIOS and IMP8 plasma instruments (Schwenn 1983). With this difficulty in mind, we summarize the average values of our three solar wind parameters (cf. Table 1) appropriate to low-speed and high-speed wind, and we indicate the smallest and largest values of the two density-dependent parameters ( $n_p u$ ,  $\rho u^2$ ) that seem consistent with the expected uncertainties in density determination. The largest values are taken from Feldman et al. (1977), and the smallest are 20% smaller (at both low and high speeds) than those given by Schwenn (1983) and correspond to the indirect inferences of solar wind proton flux density drawn from Ly- $\alpha$  backscatter observations (e.g. Lallement et al. 1985). Note that the values in Table 1 apply to a heliocentric distance of  $r = r_E = 1$  AU; in the supersonic flow beyond 1 AU,  $u$  can be assumed constant, and both  $n_p u$  and  $\rho u^2$  can be assumed to vary as  $r_E^2/r^2$ .

## 2.2 *The Very Local Interstellar Medium (VLISM)*

Our knowledge of the interstellar medium very near the solar system derives to some extent from observations of the interstellar medium (ISM)

**Table 1** Average values of solar wind parameters in high-speed and low-speed flows at  $r = r_E = 1$  AU

Wind parameter	Low-speed flows	High-speed flows
$u$ (km s <sup>-1</sup> )	330	700
$n_p u$ (cm <sup>-2</sup> s <sup>-1</sup> ) <sup>a</sup>	$3.9 \times 10^8$	$2.7 \times 10^8$
$n_p u$ (cm <sup>-2</sup> s <sup>-1</sup> ) <sup>b</sup>	$2.6 \times 10^8$	$1.6 \times 10^8$
$\rho u^2$ (dyn cm <sup>-2</sup> ) <sup>a</sup>	$2.1 \times 10^{-8}$	$3.2 \times 10^{-8}$
$\rho u^2$ (dyn cm <sup>-2</sup> ) <sup>b</sup>	$1.7 \times 10^{-8}$	$1.9 \times 10^{-8}$

<sup>a</sup> Largest expected average values (from Feldman et al. 1977).

<sup>b</sup> Smallest expected average values: 20% below those given by Schwenn (1983), as inferred by Lallement et al. (1985); note the small variation of  $\rho u^2$  (Steinitz & Eyni 1980). Uncertainties associated with electrostatic analyzer observations (Feldman et al. 1977, Schwenn 1983) may soon be substantially reduced through the analysis of Faraday cup observations during the same time period (Lazarus & Belcher 1988; A. J. Lazarus, private communication, 1989).

over very long lines of sight (namely, over distances of much more than 100 pc), but more useful information is gained from observations restricted to the local interstellar medium (LISM), which we arbitrarily define to lie within 100 pc of the Sun. Of course, the most useful information for our purposes would come from observations of the VLISM, in which the heliosphere is immersed, and which we take to lie within 0.01 pc of the Sun. Unfortunately, our observations of the VLISM are confined to the interstellar neutral gas and Galactic cosmic rays, both of which can penetrate deeply into the heliosphere, but both of whose characteristics may be significantly modified during this penetration.

The general picture of the LISM that has emerged over the last several years is thoughtfully discussed by Cox & Reynolds (1987), and it is recommended that their review be read in conjunction with the present one. We can summarize this picture of the LISM by referring to Figure 1, which is adapted from Figure 2 of Cox & Reynolds (1987). It appears that the Sun is currently located in a volume called the Local Bubble, whose dimensions range from some 70 pc across in the Galactic plane to some 300 pc across perpendicular to the Galactic plane. This volume is filled predominantly by a hot, low-density, X-ray-emitting plasma characterized by an electron density of about  $5 \times 10^{-3}$  cm<sup>-3</sup> and a temperature of about 10<sup>6</sup> K. The Sun, however, is immersed in a small-scale (a few parsecs or less) feature, called the Local Fluff, that has a much higher density, ( $\sim 10^{-1}$  cm<sup>-3</sup>) and a much lower temperature ( $\sim 10^4$  K) than the Local Bubble. It is not known whether the Local Fluff is an equilibrium or nonequilibrium structure characteristic of the Local Bubble or of an expanding Loop I Bubble (cf. Figure 1), which is thought to be the remnant of a supernova explosion.

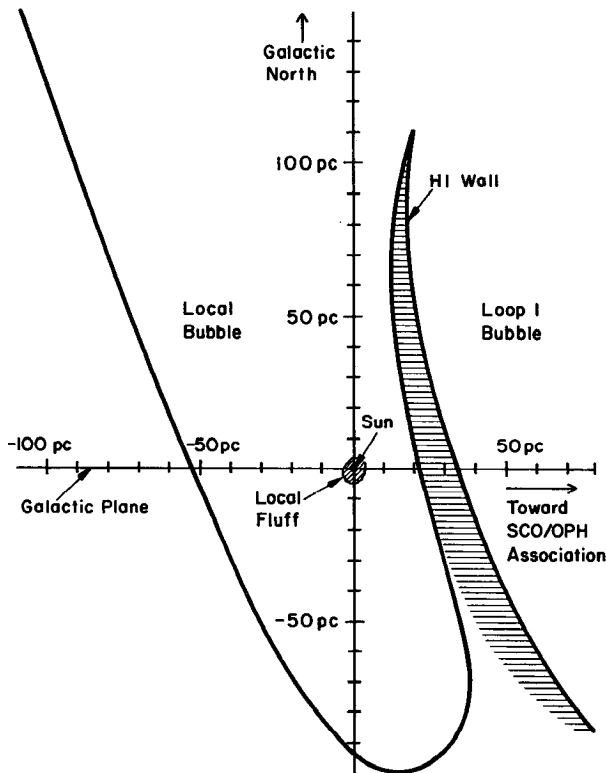


*Figure 1* A cross section of the Local Bubble in the Galactic meridional plane, the right half of which corresponds to a Galactic longitude between  $330^\circ$  and  $350^\circ$  (based on Figure 2 of Cox & Reynolds 1987). The shaded region around the Sun is the Local Fluff, in which the heliosphere is thought to be immersed. The other shaded region represents a wall of neutral hydrogen separating the Local Bubble from the Loop I Bubble.

We can, however, place significant constraints on the parameters characterizing the various components of the VLISM, and perhaps of the Local Fluff as a whole.

**2.2.1 NEUTRAL ATOMIC COMPONENT OF THE VLISM** Neutral atoms in the interstellar medium penetrate relatively freely into the heliosphere (e.g. Patterson et al. 1963, Hundhausen 1968, Blum & Fahr 1970, Holzer & Axford 1971), and solar UV radiation resonantly scattered by these atoms has been observed from space over the past two decades (e.g. early papers by Bertaux & Blamont 1971, Thomas & Krassa 1971, Paresce & Bowyer 1973; reviews by Tinsley 1971, Fahr 1974, Thomas 1978; recent papers by Chassefière et al. 1986, 1988a,b, Ajello et al. 1987, and references therein).

Extensive analyses of backscattered radiation observed in the resonance lines of H I  $\lambda$ 1216 and He I  $\lambda$ 584, coupled with models of the penetration of interstellar neutrals into interplanetary space, have led to the following inferred properties of the neutral component of the VLISM. The velocity of the VLISM relative to the Sun has a magnitude

$$u_l = 23 \pm 2 \text{ km s}^{-1}$$

and is directed toward approximately  $74.5^\circ$  ecliptic longitude and  $-7.5^\circ$  ecliptic latitude (corresponding to  $175^\circ$  Galactic longitude and  $-21^\circ$  Galactic latitude). This implies a motion of the neutral VLISM relative to the local standard of rest of about  $20 \text{ km s}^{-1}$  toward a Galactic longitude of about  $120^\circ$  and very nearly in the Galactic plane. The H I and He I densities and temperatures in the VLISM are

$$n_{\text{H}} = 0.10 \pm 0.03 \text{ cm}^{-3},$$

$$n_{\text{He}} = 0.010 \pm 0.005 \text{ cm}^{-3},$$

$$T_{\text{H}} = (9 \pm 2) \times 10^3 \text{ K},$$

$$T_{\text{He}} = (9 \pm 2) \times 10^3 \text{ K}.$$

The relatively large uncertainties in the hydrogen and helium densities reflect conflicts among different observational inferences, rather than the uncertainty estimates attached to any of the individual inferences (which are generally considerably smaller). Evidently, the ratio  $n_{\text{He}}/n_{\text{H}}$  is consistent with the cosmic value of  $[\text{He}]:[\text{H}] = 0.1$  for a rather large range of ionization fractions (cf. Blum et al. 1980, Meier 1980, Weller & Meier 1981), so inference of the ionization fraction of the VLISM from UV backscatter observations must await reduction of the density uncertainties. Values of  $u_l = 25 \text{ km s}^{-1}$ ,  $n_{\text{H}} = 0.12 \text{ cm}^{-3}$ , and  $T_{\text{H}} = 1.15 \times 10^4 \text{ K}$  inferred for the Local Fluff (Frisch 1986) lie at the high end of the ranges given above for the VLISM, and at present these two sets of observations cannot be considered inconsistent. Of course, there is no reason to believe that average values for the Local Fluff should correspond exactly to VLISM values, because the VLISM makes up only a tiny fraction of the Local Fluff volume.

**2.2.2 IONIZED, THERMAL COMPONENT OF THE LOCAL FLUFF** Since we cannot presently draw useful inferences concerning the VLISM ionization state from UV backscatter observations, we must rely on line-of-sight average values of the electron density deduced for the Local Fluff from observations of nearby stars. The results of such observations are summarized by Frisch et al. (1987) as a prelude to their discussion of a specific

study of the Local Fluff through observation of Mg I  $\lambda 2852$  in the direction of  $\alpha$  Oph. If it is assumed that in a warm gas the Mg ionization balance between the first two stages is determined by photoionization of Mg I and dielectronic recombination of Mg II, then it is possible to estimate the absorption in Mg I  $\lambda 2852$  that would be produced by the Local Fluff with a given electron density. Frisch et al. (1987) conclude that an appropriate upper limit on the electron density in the Local Fluff is  $n_e \lesssim 3 \times 10^{-3} \text{ cm}^{-3}$ , which is a factor of 5 smaller than the theoretical predictions of McKee & Ostriker (1977) when applied to a gas with temperature  $10^4 \text{ K}$  and density  $0.1 \text{ cm}^{-3}$ . Of course, the VLISM is not necessarily in the same ionization state as the Local Fluff as a whole, but it seems that the results of Frisch et al. (1987) provide a strong indication of a low VLISM electron density. For the purpose of the calculations in Section 3, we take

$$n_e < 0.1 n_H.$$

**2.2.3 THE VLISM MAGNETIC FIELD** The magnetic field is, perhaps, the most difficult of the interstellar parameters to determine. A variety of methods have been used in attempts at this determination, including the analysis of pulsar rotation and dispersion measures, the detection of the Zeeman effect, and the comparison of Galactic synchrotron emission with the Galactic cosmic-ray electron spectrum at high energies (e.g. review by Heiles 1976; more recent papers by Thompson & Nelson 1980, Brown & Chang 1983, Troland & Heiles 1986, and references therein). The most attractive result of such studies is the correlation of magnetic field with gas density suggested by Brown & Chang (1983), but unfortunately the method used in obtaining this correlation seems to be statistically invalid (Troland & Heiles 1986). Troland & Heiles (1986), using the data of Thompson & Nelson (1980) and employing reasonable assumptions about the "background" and "fluctuating" components of the Galactic magnetic field, conclude that a field of about  $5 \mu\text{G}$  is most likely to characterize a warm, low-density gas like the Local Fluff. The uncertainties in this estimate, however, are rather large, and we shall take the VLISM magnetic field to be

$$B_1 = 5 \pm 3 \mu\text{G}.$$

The parameter in which we are most interested is, of course, the magnetic pressure (cf. Section 3), and it is evidently highly uncertain, with its lower and upper bounds differing by more than an order of magnitude.

**2.2.4 GALACTIC COSMIC RAYS** Galactic cosmic rays make a significant contribution to the energy density of the ISM and thus might be expected to play an important role in the interaction between the solar wind and the

VLISM. We can observe Galactic cosmic rays directly with interplanetary spacecraft-borne detectors (e.g. Webber 1987), but the observed cosmic-ray energy spectrum is significantly modified at low energies through interaction with the expanding solar wind, so there is some uncertainty concerning the contribution to the total Galactic cosmic-ray pressure by the low-energy particles ( $< 300$  Mev nucleon $^{-1}$ ). Although it has been suggested that the low-energy cosmic rays could provide a pressure as large as  $6 \times 10^{-12}$  dyn cm $^{-2}$  (Suess & Dessler 1985), a rather thorough analysis of the problem by Axford & Ip (1986; see also Axford 1976, Ip & Axford 1985) has demonstrated that this is likely to be a substantial overestimate. Axford & Ip (1986) have considered the possibilities that we are either far from or near to (or immersed in) a supernova remnant (namely, that associated with the Loop I Bubble discussed above), and they have concluded that it is highly probable that low-energy cosmic rays make only a small contribution to the total cosmic-ray pressure. Consequently, we assume the following for our calculations in Section 3:

$$p_{\text{cr}}(\text{total}) \approx (1.3 \pm 0.2) \times 10^{-12} \text{ dyn cm}^{-2},$$

$$p_{\text{cr}}(< 300 \text{ Mev nucleon}^{-1}) \approx (3 \pm 2) \times 10^{-13} \text{ dyn cm}^{-2}.$$

2.2.5 INTERSTELLAR DUST We assume (e.g. Greenberg 1978) that dust in the VLISM has a typical grain radius of  $0.05 \mu\text{m}$ , which is appropriate for metallic grains, and that the dust-to-gas ratio by mass is 0.01, leading to a mass density for dust of

$$\rho_d \approx 2 \times 10^{-27} \text{ g cm}^{-3}.$$

### 2.3 Interaction Between the Solar Wind and the VLISM

The only relatively direct observational evidence we have of the interaction between the solar wind and the VLISM involves the penetration of interstellar neutral atoms and Galactic cosmic rays into interplanetary space, which we discussed above (cf. Sections 2.2.1, 2.2.4). The observation most relevant to the basic dynamical wind/VLISM interaction would be detection of the shock front expected to characterize the transition from supersonic to subsonic solar wind flow. As yet, there has been no certain detection of this shock, but there are three lines of observational evidence that are currently thought to point to a location of the shock just outside the orbit of Pluto.

The first of these involves the detection, beginning in late 1983, of radio frequency signals near 2 and 3 kHz by the *Voyager 1* and 2 plasma wave instruments (Kurth et al. 1984, 1987, Kurth 1988). At the time of first detection, the ambient solar wind plasma frequency was below the

observed frequency range, so the signals could be interpreted as resulting from freely propagating radio waves in the outer heliosphere. Before the separate spectral peaks at 2 and 3 kHz were resolved, Kurth et al. (1984) suggested the possible interpretation that these radio waves were generated by the shock terminating supersonic solar wind flow at twice the downstream plasma frequency. A plasma frequency between 1 and 1.5 kHz corresponds to a downstream electron density between 0.012 and 0.028  $\text{cm}^{-3}$  and (for a strong shock) to an upstream density between 0.003 and 0.007  $\text{cm}^{-3}$ . Extrapolating this density range back to 1 AU, assuming a constant solar wind flow speed, we see from Table 1 that it corresponds to a range of shock distances  $34 \text{ AU} < R_s < 63 \text{ AU}$  for low-speed flows and to a range  $18 \text{ AU} < R_s < 36 \text{ AU}$  for high-speed flows.

The existence of two separate spectral peaks with a frequency ratio of 1.6 (eliminating the possibility of harmonic emission) complicates the interpretation. One suggested resolution (Lee 1988) is that the two frequencies correspond to twice the plasma frequencies upstream and downstream of a shock [modified by cosmic-ray pressure (Lee & Axford 1988, Drury 1988)], with a density jump of 2.56 rather than 4. This interpretation leads to shock distances of  $25 \text{ AU} < R_s < 31 \text{ AU}$  for low-speed flows and  $14 \text{ AU} < R_s < 18 \text{ AU}$  for high-speed flows. These values are a bit too small, since a shock in these distance ranges would already have been crossed by deep space probes. Another possible interpretation of the two spectral peaks (Kurth et al. 1987) involves a modification of the first (Kurth et al. 1984) interpretation through the assumption of an asymmetric termination shock, with the two different frequency bands originating from two different regions of the shock; we return to a discussion of this possibility in Section 3. Finally, McNutt (1988) has recently suggested that the radio emissions are triggered by two anomalous high-speed solar wind streams, and he places the shock distance in the range  $70 \text{ AU} < R_s < 140 \text{ AU}$ . The detailed arguments underlying this hypothesis will have to be worked out before its viability can be evaluated.

A second line of evidence indicating a not-too-distant termination shock is based on a combination of observations of the cosmic-ray anomalous component (e.g. Cummings & Stone 1988) and theoretical models of the acceleration of the anomalous component (Pesses et al. 1981, Fisk 1986, Jokipii 1986; L. A. Fisk, unpublished work, 1982) through the injection and first-order Fermi acceleration of interstellar pickup ions (cf. Section 3.6) at the termination shock (see the review by Lee 1988). The cosmic-ray anomalous component is thought to arise from the ionization of interstellar neutral atoms, which implies that it consists of energetic singly charged atoms, in contrast to the highly charged atoms making up most of the cosmic-ray spectrum. If the anomalous component does originate

from interstellar neutral atoms that are ionized in the solar wind, then hydrogen (which is not detected as part of the anomalous component, presumably because of obscuration by Galactic cosmic-ray protons) should dominate the anomalous component pressure. Observations, together with the inferred presence of hydrogen, indicate that the anomalous component pressure is increasing sufficiently rapidly out to 20 AU that it is likely to be comparable to the solar wind ram pressure inside 50 AU if the anomalous component is accelerated at the termination shock [Cummings & Stone 1988 (these authors do, however, present evidence that the anomalous component pressure may not increase as rapidly outside 20 AU as it does nearer the Sun)]. Evidently, if this is the case, the shock location must be  $R_s < 50$  AU.

Another inference of a termination shock inside 50 AU comes from observations of H I  $\lambda 1216$  radiation scattered by interstellar hydrogen atoms that have penetrated into interplanetary space. The *Pioneer 10* Ly- $\alpha$  data apply to the downstream direction (with respect to the interstellar wind) in which the spacecraft is traveling, and it shows an anomalously rapid decrease in backscattered Ly- $\alpha$  beyond about 39 AU (Wu et al. 1988). This decrease is interpreted as a possible signature of a nearby termination shock, beyond which the relatively high-density, high-temperature subsonic solar wind flow produces a more rapid ionization of interstellar H atoms. It is not clear, however, how the relatively sharp drop in Ly- $\alpha$  intensity beyond 39 AU can be consistent with a shock-related decline in hydrogen density, which we would expect to be relatively gradual. At present, therefore, we resist the temptation to take this UV observation as an indication of a termination shock inside 50 AU.

### 3. MODELS OF THE INTERACTION BETWEEN THE SOLAR WIND AND THE INTERSTELLAR MEDIUM

The dynamical interaction between the solar wind and the interstellar medium involves the relaxation toward pressure equilibrium between the solar and interstellar magnetized plasmas. This relaxation is characterized principally by the transition from supersonic to subsonic solar wind flow (presumably a shock transition, which we refer to as the terminal shock) and by the turning of the subsonic solar wind flow to achieve compatibility with the local interstellar structure. As mentioned in Section 1, the location of the terminal shock is currently of particular interest because of the prospect of one or more spacecraft crossing it in the near future. In attempting to determine the most likely location for the terminal shock, not only must we consider the ram pressure of the supersonic solar wind

and the pressure of the interstellar medium into which the wind is expanding, but we must also examine the structure of the postshock subsonic solar wind flow.

Basic to our study of this dynamical interaction is the understanding of mass and momentum balance in a magnetized fluid, which are described by

$$\frac{\partial \rho}{\partial t} + \nabla \cdot (\rho \mathbf{u}) = 0, \quad 1.$$

$$\frac{\partial}{\partial t} (\rho \mathbf{u}) + \nabla \cdot (\rho \mathbf{u} \mathbf{u}) + \nabla p + \nabla (B^2/8\pi) - (\mathbf{B} \cdot \nabla) (\mathbf{B}/4\pi) = \mathbf{F}, \quad 2.$$

where  $\rho$ ,  $\mathbf{u}$ , and  $p$  are the mass density, flow velocity, and thermal pressure of the fluid, respectively;  $\mathbf{B}$  is the magnetic field; and  $\mathbf{F}$  includes the effects of body forces, such as gravitational, radiative, and frictional forces. We consider below mass and momentum balance both along a streamline in a subsonic flow and across interfaces (either a shock front separating the supersonic and subsonic flow regimes of a fluid or a contact surface separating two nonpenetrating fluids). Across an interface that is parallel to the local magnetic field and perpendicular to the local flow velocity (i.e. for which  $\mathbf{B} \cdot \hat{\mathbf{n}} = 0$  and  $\mathbf{u} \times \hat{\mathbf{n}} = \mathbf{0}$ , where  $\hat{\mathbf{n}}$  is the unit vector normal to the surface), we see from Equation 2 that in a steady state the total pressure is conserved, i.e.

$$\rho u^2 + p + B^2/8\pi + p_F = \text{constant}, \quad 3a.$$

where the total pressure is the sum of the four terms on the left side of Equation 3a, which represent (from left to right) the ram pressure (normal to the surface), the thermal pressure, the magnetic pressure, and the pressures ( $p_F$ ) associated with the ambient media (e.g. neutral gas and cosmic rays) producing a frictionlike interaction. In a flow that is highly supersonic and super-Alfvénic, like the supersonic solar wind, the ram pressure is much larger than the thermal and magnetic pressures, whereas in a very subsonic or sub-Alfvénic flow, the ram pressure is negligible. Evidently, Equation 3a applies to an interface (like a shock front) across which there is a flow of mass. For a contact surface across which mass does not flow (i.e.  $\mathbf{u} \cdot \hat{\mathbf{n}} = 0$ ), the ram pressure term in Equation 3a disappears and pressure balance across the surface is described by

$$p + B^2/8\pi + p_F = \text{constant}. \quad 3b.$$

The above descriptions of mass and momentum balance are, of course, incomplete without either a description of energy balance or the imposition

of some other condition (e.g. the assumption of incompressibility), and we consider such additional requirements below as the need arises.

Our approach to the following theoretical discussion is guided by Parker's (1961, 1963) description of three fundamental types of interaction between stellar and interstellar plasmas. First, we discuss Parker's results in Sections 3.1–3.3, and then we go on to consider modifications of these results brought about through the effects of the solar magnetic field, the interstellar neutral gas, cosmic rays, and interstellar dust (Sections 3.4–3.7). Finally, in Section 3.8, we conclude by describing the expected structure of the heliospheric cavity formed through the interaction between the solar wind and the interstellar medium.

### 3.1 *Static, Unmagnetized Interstellar Plasma*

Let us first consider a steady, radial, spherically symmetric solar wind interacting with a static, unmagnetized interstellar plasma (Parker 1963). In the asymptotic flow regime of the supersonic solar wind, the flow speed  $u$  is nearly constant, so according to Equation 1 the density  $\rho$  and the ram pressure  $\rho u^2$  decline as  $1/r^2$ , where  $r$  is the heliocentric radial distance. Beyond some distance  $R_t$  the ram pressure of the supersonic wind falls below the interstellar pressure  $p_t$ , and the solar wind can no longer stand off the interstellar medium (cf. Equation 3): Evidently,  $R_t$  is given by

$$R_t = (\rho_E u_E^2 / p_t)^{1/2}, \quad 4.$$

where  $R_t$  is measured in astronomical units, and the subscript E refers to wind parameters at  $r = 1$  AU. In essence, near the distance  $R_t$  the supersonic solar wind encounters an interstellar barrier and must undergo a shock transition to a subsonic flow (Clauser 1960, Weymann 1960), which can achieve pressure equilibrium with the interstellar medium. If we assume a strong, adiabatic shock with an adiabatic index (ratio of specific heats) of  $5/3$ , the Rankine-Hugoniot relations [i.e. the equations of mass, momentum, and energy conservation across the shock (cf. Equation 3)] yield the following relations between parameters just upstream (subscript s1) and just downstream (subscript s2) of the shock:

$$u_{s1}/u_{s2} = \rho_{s2}/\rho_{s1} = 4, \quad 5.$$

$$p_{s2} = 3\rho_{s1}u_{s1}^2/4, \quad 6.$$

where the magnetic field is neglected (a good approximation in a highly super-Alfvénic flow). In the postshock subsonic region the flow speed declines quite rapidly, and in the absence of a magnetic field (see Section 3.4 for a discussion of magnetic effects in the subsonic region) the flow is very nearly incompressible, so that  $\mathbf{u} \cdot \nabla \rho = \nabla \cdot \mathbf{u} = 0$ . It then follows from

Equation 2 that a constant of the subsonic flow is  $\rho u^2/2 + p (= \rho_{s2} u_{s2}^2/2 + p_{s2})$ . The rapid decline of the flow speed leads to a dominance of the thermal pressure in the subsonic flow (i.e.  $p \gg \rho u^2/2$ ), so near the heliopause (the boundary of the heliosphere) we have  $p \approx \rho_{s2} u_{s2}^2 + p_{s2}$ . It follows from Equation 3b that the interstellar pressure  $p_i$  must equal  $\rho_{s2} u_{s2}^2/2 + p_{s2}$ . Hence, using Equations 5 and 6 we can relate the shock location  $R_s$  (measured in astronomical units) to the solar wind ram pressure and interstellar pressure by

$$R_s = (7\rho_E u_E^2/8p_i)^{1/2}, \quad 7.$$

where we have assumed that  $\rho u^2 \propto r^{-2}$  in the supersonic solar wind. As we should expect, comparison of Equations 4 and 7 indicates that  $R_t$  and  $R_s$  are essentially the same.

Our heliosphere, in this simplest of possible models, is thus characterized by a spherical shock transition at  $R_s$  and a spherical heliopause boundary (separating the solar and interstellar plasmas, which are assumed not to interpenetrate) that is very slowly moving outward at a speed  $u = u_{s2}(R_s/R)^2$ . Evidently, the heliopause radius is a function of time, the solar wind flow speed, and the shock radius, and it can be written

$$r_H = 0.4 \left[ \left( \frac{u_E}{4 \times 10^7} \right) \left( \frac{R_s}{100} \right)^2 \left( \frac{t}{10^9} \right) \right]^{1/3} \text{ pc}, \quad 8.$$

where the units of  $u_E$ ,  $R_s$ , and  $t$  are centimeters per second, astronomical units, and years, respectively. Over the lifetime of the Sun, assuming a steady solar wind, the heliopause boundary reaches a distance on the order of 1 pc from the Sun. Of course, any flow of the interstellar medium relative to the Sun must drastically modify the shape of this vast region of subsonic solar wind flow, and this is the subject we next address.

### 3.2 *Flowing, Unmagnetized Interstellar Plasma*

Let us again consider unmagnetized solar and interstellar plasmas that do not interpenetrate and whose regions of subsonic flow can be approximately treated as incompressible. A flow of the interstellar plasma relative to the Sun produces an asymmetry in the total interstellar pressure, with the maximum pressure exerted at the heliopause along the stagnation line, which runs radially outward from the Sun in the direction upstream in the interstellar wind (cf. Figure 2). This asymmetry of the total interstellar pressure leads to an asymmetry of the terminal shock, with the minimum shock distance occurring along the stagnation line. The resultant deviation of the shock normal from the radial direction produces (at the shock) a turning of the flow away from the stagnation line, which leads to the

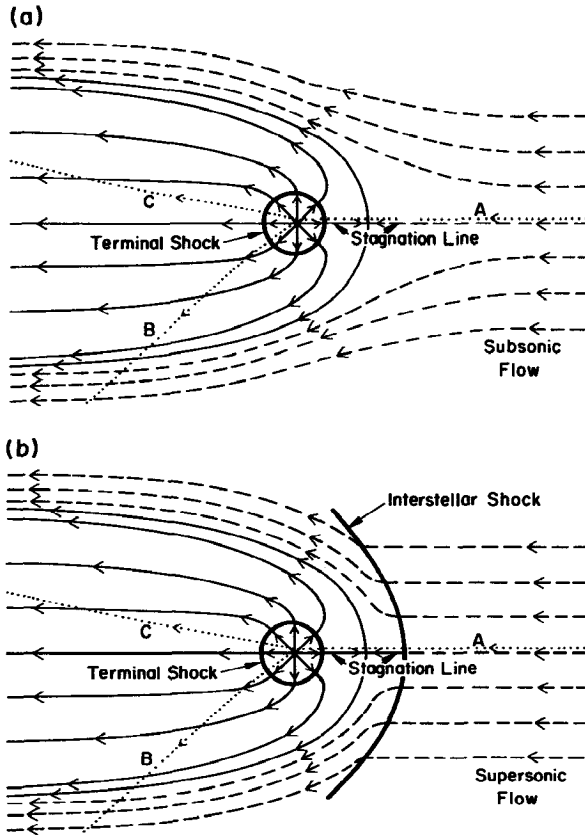


*Figure 2* Schematic description of the noninterpenetrating interaction of a flowing, unmagnetized interstellar plasma with an unmagnetized solar wind for the cases in which the interstellar plasma flow relative to the Sun is (a) subsonic (adapted from Parker 1963) and (b) supersonic [adapted from Baranov et al. (1970) and Parker (1963)]. The curves with arrows are flow lines of the solar (solid) and interstellar (dashed) plasmas. The solid curves without arrows represent the shock front terminating supersonic solar wind flow (panels a and b) and the bow shock (panel b) standing in front of the heliosphere through which the supersonic interstellar flow passes. The dotted curves are trajectories of an interstellar hydrogen atom that is subjected to either a net attractive force (curve AB) or a net repulsive force (curve AC), where the net force is the sum of the solar gravitational force and Ly- $\alpha$  radiation force.

eventual alignment of the postshock subsonic solar wind flow with the interstellar gas flow (as is illustrated in Figure 2).

The flow of the interstellar gas relative to the Sun may be either subsonic (Parker 1963) or supersonic (Baranov et al. 1970, 1976), and the form of the interstellar stagnation pressure  $\pi_1$  is different in these two cases. In the subsonic case ( $u_1^2 < 5\rho_1/3\rho_1$ ), it is just

$$\pi_1 = p_1 + \frac{1}{2}\rho_1 u_1^2, \quad 9.$$

which is what we would expect from the discussion in Section 3.1. In the supersonic case ( $u_1^2 > 5p_1/3\rho_1$ ), the interstellar gas must pass through a standing bow shock in front of the heliosphere (cf. Figure 2*b*), and the stagnation pressure becomes

$$\pi_1 = \frac{3}{8}p_1 + \frac{7}{8}\rho_1 u_1^2, \quad 10.$$

where  $\rho_1$ ,  $u_1$  and  $p_1$  are preshock parameters. In either case, the solar wind stagnation pressure remains  $p_2 + \rho_2 u_2^2/2$ , so the terminal shock position along the stagnation line is given by Equation 7, with  $p_1$  replaced by  $\pi_1$ .

### 3.3 *Magnetically Dominated, Static Interstellar Plasma*

In examining the effect of an interstellar magnetic field, let us return to the consideration of a static interstellar plasma (cf. Section 3.1), which this time includes an interstellar magnetic field whose energy density is much larger than that of the other component(s) of the interstellar medium. Such a field can be described in terms of a scalar potential and is characterized by the balance between the magnetic tension and magnetic pressure gradient forces. If a spherical body that excludes magnetic field is inserted into an otherwise uniform interstellar field, the field outside the spherical body remains potential and can be described by (Parker 1963)

$$\psi_1 = -B_0(r + a^\beta/(\beta - 1)r^{\beta-1}) \cos \theta, \quad 11.$$

$$\mathbf{B}_1 = -\nabla\psi_1 = B_0[\hat{\mathbf{e}}_r(1 - a^\beta/r^\beta) \cos \theta - \hat{\mathbf{e}}_\theta(1 + a^\beta/(\beta - 1)r^\beta) \sin \theta], \quad 12.$$

where  $\psi_1$  is the magnetic scalar potential,  $\hat{\mathbf{e}}_r$  and  $\hat{\mathbf{e}}_\theta$  are unit vectors,  $r$  is measured from the center of the excluding sphere,  $\theta = 0$  is the direction of the undisturbed interstellar field, and  $\beta = 3$ . If a cylinder, rather than a sphere, excludes the interstellar field, then Equations 11 and 12 still apply, but now  $\beta = 2$ .

The distorted interstellar field, whose lines of force are defined by  $(a/r)[(r/a)^\beta - 1] \sin^{\beta-1} \theta = \text{constant}$ , is illustrated in Figure 3, where seven field lines (one the  $\theta = 0$  field line) that are equally spaced as  $r \rightarrow \infty$  (namely,  $r \sin \theta \rightarrow 0, \pm a/2, \pm a, \pm 3a/2$ ) are drawn in the  $r$ - $\theta$  plane for both the sphere (panel *a*) and the cylinder (panel *b*). Evidently, the distortion leads to an enhanced interstellar magnetic pressure ( $B_1^2/8\pi$ ), which maximizes for  $\theta = \pi/2$ . The largest enhancement occurs at the surface of the excluding sphere or cylinder ( $r = a$  and  $\theta = \pi/2$ ), where the interstellar magnetic pressure is a factor of 2.25 (4.0) larger than its value far from the sphere (cylinder). Of course, at the two points  $r = a, \theta = 0, \pi$  the magnetic pressure vanishes; the implications of this effect are discussed in

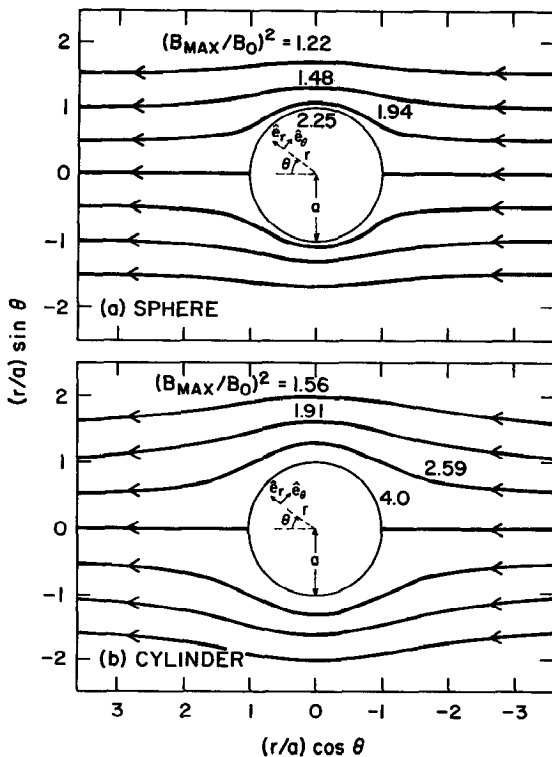


Figure 3 Potential magnetic field lines of an interstellar field distorted by either a spherical (panel *a*) or a cylindrical (panel *b*) heliospheric cavity of radius  $a$  that excludes magnetic field. The maximum enhancement of the magnetic pressure along each field line (which occurs at  $\theta = 90^\circ$ ) is given. For a spherical cavity the field is symmetric about the  $\theta = 0^\circ$  line, and for a cylindrical cavity the field is symmetric about the  $\theta = 0^\circ$  plane. Here  $r$  and  $\theta$  are two of the three coordinates of either a spherical or a cylindrical coordinate system (adapted from Parker 1963).

Sections 3.4 and 3.8, where the consequences of a heliospheric magnetic field are considered.

Clearly, when the magnetic field provides a significant contribution to the total interstellar pressure, we must consider the consequences of the heliospheric distortion of the interstellar magnetic field, and this is done in Section 3.8. Before proceeding, however, we note that any of the magnetic surfaces (cf. Figure 3) that are symmetric about the line  $\theta = 0^\circ$  (spherical case) or about the plane perpendicular to the paper and including the line  $\theta = 0^\circ$  (cylindrical case) can be considered the boundary of a region from which the interstellar magnetic field is excluded (i.e. the heliospheric bound-

ary). Parker (1963) made use of this fact in his discussion of the outflow of the subsonic solar wind along the direction of the interstellar magnetic field, a subject to which we return in Sections 3.4, 3.5, and 3.8.

### 3.4 *Effects of a Heliospheric Magnetic Field*

The solar magnetic field is drawn out from the Sun by the radially expanding supersonic solar wind, and owing to solar rotation the magnetic field takes the form (on average) of an Archimedes spiral (Parker 1958, 1963), i.e.

$$B_{\phi}/B_r = (4.3 \times 10^7/u)R \sin \theta, \quad 13.$$

where  $\phi$  and  $\theta$  are solar azimuth and colatitude, and the units of  $u$  and  $R$  are centimeters per second and astronomical units, respectively. Evidently, by the time the solar wind reaches the terminal shock ( $R \gtrsim 50$  AU) the magnetic field is very nearly azimuthal, except at the highest solar latitudes (cf. Equation 13). For the purpose of the following discussion, we assume that the field is purely azimuthal at and beyond the terminal shock.

As noted above, in the supersonic solar wind the magnetic energy density is negligible ( $\lesssim 1\%$ ) in comparison with the total wind energy density. Across the terminal shock, the magnetic pressure increases by no more than a factor of 16 (for a strong shock) and thus remains small ( $< 15\%$ ) in comparison with the gas pressure just downstream of the shock. Hence, as assumed above, the postshock flow is initially very nearly incompressible, which requires that  $u$  decrease nearly as  $r^{-2}$ . Yet  $B \propto (ur)^{-1} \propto r$ , so if nearly spherically symmetric subsonic flow extends to a great enough radial distance (which depends on the interstellar neutral gas interactions discussed in Section 3.5), the magnetic energy density becomes dominant, and the magnetic field controls the structure of the flow (e.g. Holzer 1972). In the region of magnetic control of spherically symmetric flow, the magnetic tension and pressure gradient forces nearly balance, so that  $B \propto r^{-1}$ , which leads to  $u = \text{constant}$  and  $n \propto r^{-2}$ . Clearly, the magnetic control of the subsonic flow leads to a decrease with radial distance of the total pressure (e.g. Cranfill 1971, Holzer 1972), and Lee (1988) has argued that this reduction may be significant in determining the terminal shock location [leading, of course, to a smaller shock distance than would be predicted on the basis of the assumption of incompressible flow (cf. Sections 3.1 and 3.2)].

Another important consequence of the magnetic energy density becoming significant in the outer heliosphere involves the structure of the heliospheric boundary (the heliopause) when the interstellar magnetic field dominates the interstellar pressure. Let us consider a situation in which the subsonic solar wind flow is turned (cf. Sections 3.2, 3.5, and 3.8) in a

direction perpendicular to the interstellar magnetic field, so that the bulk of the heliosphere takes the shape of the cylinder illustrated in Figure 3*b*. As noted in Section 3.3, the pressure exerted by the interstellar magnetic field at this boundary decreases substantially from the direction perpendicular to the direction parallel to the interstellar field. If the subsonic solar wind flow were incompressible, then pressure balance at the heliopause would require a substantial distortion of this cylindrical shape, with the heliosphere expanding parallel to the interstellar field and contracting perpendicular to the field until a heliopause shape nearer that described by the outermost interstellar field lines shown in Figure 3*b* were achieved. Such a shape would clearly be associated with very little enhancement of the interstellar magnetic pressure (cf. Figure 3*b*) through field distortion resulting from the presence of the heliospheric cavity.

The situation is different, however, if the heliospheric magnetic field is dominant near the heliopause, and the heliospheric field has a significant component in the plane of the paper in Figure 3. This situation is illustrated schematically in Figure 4 (which is a modification of Figure 3), where the heliospheric field is assumed to be circular near the terminal shock and to lie in the plane perpendicular to the axis of the cylinder. Although the heliosphere is distorted from its cylindrical shape, the distortion is relatively minor (owing to the tension of the heliospheric field), and the enhancement of the interstellar magnetic pressure remains relatively large. Note that in the region where the heliopause bulges, the heliospheric

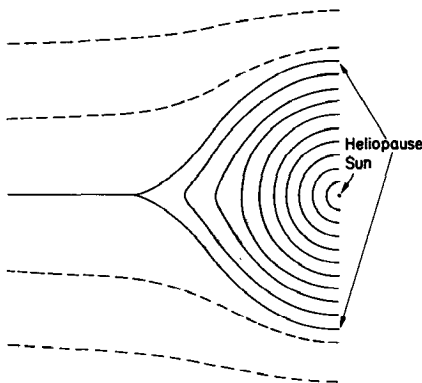


*Figure 4* Schematic illustration of the adjustments of the heliospheric and interstellar magnetic fields when the heliospheric cavity is no longer a cylinder (cf. Figure 3), but instead the heliospheric field is taken to be nearly circular near the Sun and potential beyond. Heliospheric field lines are solid, and interstellar field lines are dashed. The spacing of the heliospheric field lines is not intended to indicate field intensity, which declines as  $r^{-1}$  near the Sun and much more rapidly near the cusp region.

pressure has decreased below its value at the heliopause in the region near the interstellar magnetic pressure maximum, so that the effect of the interstellar pressure enhancement on the terminal shock distance along flow lines intersecting each region should be essentially the same. We return to this discussion of heliospheric structure, as well as the possible effects of magnetic field line reconnection, in Section 3.8.

### 3.5 *Effects of a Flowing Interstellar Neutral Gas*

As indicated in Figure 2, the interstellar neutral gas penetrates relatively freely into the heliosphere. The neutral atoms, particularly H and He, resonantly scatter solar radiation, so that the distribution of interstellar H and He in the heliosphere can be studied by observing sky background radiation in H I  $\lambda 1216$  and He I  $\lambda 584$ . Such studies, coupled with models for the penetration of interstellar neutrals into the heliosphere (Section 3.5.1), allow inferences to be drawn concerning the thermodynamic parameters of the neutral component of the VLISM (cf. Section 2.2). Interstellar neutrals penetrating the heliosphere lead to significant modifications of both the thermal plasma and the energetic particle population in the heliosphere. They slow and heat the supersonic solar wind (Section 3.5.2) and in so doing provide a population of seed particles that can be accelerated at the terminal shock to produce low-energy cosmic rays (Section 3.6.2). Interstellar neutrals also both cool and turn the subsonic solar wind flow and thus play an important role in determining the structure and location of both the terminal shock and the heliopause (Sections 3.5.3 and 3.8).

#### 3.5.1 PENETRATION OF INTERSTELLAR NEUTRALS INTO THE HELIOSPHERE

Two possible orbits of a hydrogen atom moving toward the heliosphere with a velocity equal to the interstellar flow velocity and an impact parameter (relative to the Sun) of about 2 AU are shown by the dotted trajectories in Figure 2. Both AB and AC are hyperbolic trajectories, the first corresponding to solar minimum conditions (for which the repulsive solar Ly- $\alpha$  radiation force is smaller than the attractive force of gravity) and the second to solar maximum conditions (for which the Ly- $\alpha$  radiation force exceeds gravity, leading to a net radially outward force on the incoming atom). Since the hydrogen atom travels about 4 AU in a year, the time to traverse the portions of trajectories AB and AC that are shown in Figure 2 is about 200 yr (assuming both that the atom is not ionized in its close encounter with the Sun and that the minimum Sun-heliopause distance is about 100 AU). The real trajectory of an interstellar atom is not smooth like trajectories AB and AC because of the significant variation of the Ly- $\alpha$  radiation force on time scales comparable to and smaller than

the time over which the net solar force has a significant effect on the trajectory (e.g. Vidal-Madjar 1977). In addition, the nonnegligible thermal speeds characterizing the interstellar neutral velocity distributions (about  $10 \text{ km s}^{-1}$  for H I and  $5 \text{ km s}^{-1}$  for He I, corresponding to  $T_1 = 10^4 \text{ K}$ ) imply that the incoming neutral atom velocity vector will not generally be closely aligned with the interstellar flow velocity, as it is assumed to be for the illustrative trajectories shown in Figure 2.

Before a hydrogen atom can complete a heliosphere-penetrating trajectory like those shown in Figure 2, it must overcome three obstacles. The first obstacle is the diverging flow of the interstellar ionized gas as it passes the heliosphere. Resonance charge transfer between interstellar hydrogen atoms and protons near the heliosphere can lead to a diversion of some fraction of the neutral gas away from the heliosphere, because through the charge transfer the neutral atom and proton effectively exchange trajectories (Wallis 1975, 1978, 1981, 1984). The region in which this diversion takes place depends on whether the interstellar gas is flowing subsonically (Figure 2a) or supersonically (Figure 2b), and it is characterized by the divergence of the interstellar plasma flow lines from the stagnation line. For subsonic flow (actually subcritical flow, where the critical speed is the hydromagnetic fast mode speed), which is likely the relevant case (cf. Section 3.8), this diversion region extends one to two times the minimum Sun-heliopause distance ahead of the heliosphere. For a charge transfer cross section of  $5 \times 10^{-15} \text{ cm}^2$  [appropriate to a 1-eV interaction energy; the cross section decreases to  $2 \times 10^{-15} \text{ cm}^2$  for a 1-keV interaction energy (Tawara et al. 1983)], only a fraction of a percent of hydrogen atoms charge exchange if the proton density is  $0.01 \text{ cm}^{-3}$  (cf. Section 2.2.2), and the minimum Sun-heliopause distance ( $R_H$ ) is on the order of 100 AU. If the product of the proton density and the Sun-heliopause distance is increased by a factor of 10, then some 30% of the hydrogen atoms charge exchange in the diversion region. Using rather large numbers for the interstellar proton density and the size of the heliosphere, and assuming that a charge transfer implies exclusion of a hydrogen atom from the heliosphere, Ripken & Fahr (1983) have suggested that a significant fraction of interstellar hydrogen atoms are diverted away from the heliosphere. Wallis (1978, 1981, 1984), however, has pointed out that in this particular case the charge transfer process corresponds more closely to a scattering process than to an extinction process, which Ripken & Fahr (1983) have implicitly assumed. The scattering process can be visualized by realizing that the charge transfer effectively produces a new population of interstellar neutrals with the same velocity distribution as the interstellar protons. The exclusion of neutral particles from the heliosphere can then be estimated by comparing the fraction of the newly produced neutral

distribution that enters the heliosphere ( $\langle f_1 \rangle$ ) with the fraction of the original neutral distribution ( $\langle f_0 \rangle$ ) that enters. It follows that the interstellar neutral hydrogen density is effectively reduced (through exclusion from the heliosphere by charge transfer) by a factor

$$F = 1 - [1 - (\langle f_1 \rangle / \langle f_0 \rangle)] (1 - e^{-\tau_H}), \quad 14.$$

$$\tau_H = \beta n_c L, \quad 15.$$

where  $n_c$  is in  $\text{cm}^{-3}$ ,  $L$  (in astronomical units) is twice the minimum Sun-heliopause distance ( $R_H$ ),  $(1 - e^{-\tau_H})$  is the fraction of atoms undergoing charge transfer, and, in the case at hand,  $\beta = 5 \times 10^{-2}$ . Since the interstellar flow speed is only a factor of 2 greater than the thermal speed, and since the diversion of the interstellar plasma is relatively gradual (cf. Figure 2), it follows that  $[1 - (\langle f_1 \rangle / \langle f_0 \rangle)] \lesssim 0.15$  and, even for the parameters of Ripken & Fahr (1983), that  $F \gtrsim 0.95$  (for the parameters given in Sections 2.2.2 and 3.8, it follows that  $F > 0.99$ ).

The second obstacle an interstellar hydrogen atom penetrating the heliosphere faces is charge transfer in the postshock subsonic solar wind. Such charge transfer produces a population of hot hydrogen atoms (formerly solar wind protons) characterized by the subsonic solar wind temperature, which is on the order of  $1.5 \times 10^6$  K near the terminal shock and decreases gradually with distance from the shock (cf. Section 3.5.3). The scattering process is the same as described in the preceding paragraph, with newly produced atoms taking on the velocity distribution of the protons, which in this case is taken to be a Maxwellian distribution essentially at rest rather than a rapidly drifting Maxwellian. We thus have a larger exclusion factor,  $[1 - (\langle f_1 \rangle / \langle f_0 \rangle)] \lesssim 0.4$ , and if we choose appropriate representations of  $\beta$ ,  $n_c$ , and  $L$ , Equation 15 becomes

$$\tau_H \approx (9/R_s) [(R_H - R_s)/R_s], \quad 16.$$

where  $R_s$  is the minimum shock distance. Taking  $R_H/R_s = 2$ , we find from Equations 14 and 16 that  $F \gtrsim 0.90$  for  $R_s = 50$  AU, and  $F > 0.95$  for  $R_s = 100$  AU. We must remember, though, that the newly produced atoms in this case have relatively high speeds ( $> 100 \text{ km s}^{-1}$ ) and will generally have radial velocity components large enough to shift them into the wings of the solar Ly- $\alpha$  line, thus making them less visible in Ly- $\alpha$  backscatter observations than are interstellar atoms (which have much lower speeds). For the purpose of interpreting Ly- $\alpha$  observations, therefore, it is more appropriate to take  $F \gtrsim 0.85$  for  $R_s = 50$  AU and  $F \gtrsim 0.93$  for  $R_s = 100$  AU.

The final obstacle faced by an interstellar hydrogen atom penetrating the heliosphere is the supersonic solar wind, in which the charge transfer

process produces a hydrogen atom traveling nearly radially outward from the Sun at the solar wind speed. Such an atom is Doppler shifted so far from the solar Ly- $\alpha$  line center as to become essentially invisible. For our purposes here, therefore, this hydrogen atom can be considered destroyed, so  $f_1 = 0$  and Equations 14 and 15 become

$$F = e^{-\tau_H}, \quad 17.$$

$$\tau_H = 5 \times 10^{-7} \int ds (2.5 \times 10^{-15} nu + 9 \times 10^{-8} r_E^2 / r^2), \quad 18.$$

where the integration is carried out along the trajectory of an interstellar hydrogen atom inside the terminal shock (the units of  $s$  are centimeters),  $nu$  is the solar wind proton flux density (in square centimeters per second), and the second term in the integrand arises from photoionization. For a hydrogen atom traveling radially inward (toward the Sun) the penetration distance (where  $\tau_H = 1$ ) is

$$R(\tau_H = 1) = \left\{ \left[ 4.5 \left( \frac{n_E u_E}{3 \times 10^8} \right) + 0.7 \right]^{-1} + R_s^{-1} \right\}^{-1} \text{ AU}, \quad 19.$$

which is about 5 AU. In contrast, interstellar helium atoms (for which the primary destruction process is photoionization rather than charge transfer) penetrate to about 0.6 AU (Holzer & Axford 1971).

In the preceding discussion, we have not considered the effects of scattering (through charge transfer in H-H<sup>+</sup> collisions and through polarization interaction in He-H<sup>+</sup> collisions) on the flow speed and temperature of the interstellar neutral gas that are inferred from UV backscatter observations (cf. Section 2.2.1). Yet when such effects are ignored, there exists a significant discrepancy between the inferred hydrogen and helium temperatures [ $0.4 \lesssim T_H/T_{He} \lesssim 0.7$  (Bertaux et al. 1977, 1985, Ajello 1978, Weller & Meier 1981, Dalaudier et al. 1984)]. A number of different treatments of the scattering have been used to produce a wide variety of conflicting results (e.g. Wallis 1978, 1984, 1988, Wallis & Hassan 1978, Wallis & Wallis 1979, Fahr et al. 1985, Chassefiere et al. 1986, 1988a,b, Chassefiere & Bertaux 1987a,b). In selecting the interstellar parameters presented in Section 2.2.1, we have relied primarily on the analysis of Chassefiere et al. (1988a,b).

**3.5.2 EFFECTS OF NEUTRALS ON THE SUPERSONIC SOLAR WIND FLOW**  
 Charge transfer collisions between interstellar hydrogen atoms and solar wind protons in the supersonic flow regime occur principally outside  $R = 5$  AU (Equation 19), where the magnetic field is nearly perpendicular to the solar wind flow (except at high solar latitudes). Thus, a newly produced

proton resulting from charge transfer experiences an electric force (associated with solar wind flow perpendicular to the local magnetic field) that accelerates it to an energy approximately twice that of an ambient solar wind proton. Immediately after attaining this energy, the motion of the newly produced proton (which we refer to as a pickup proton or, generically, as a pickup ion) can be described as the superposition of an outward radial motion at the solar wind speed and a circular motion (also characterized approximately by the solar wind speed) in the solar wind rest frame in a plane perpendicular to the local magnetic field. The motion of a newly produced neutral atom is, of course, just an outward radial motion at the solar wind speed. The net effect on the solar wind of a charge transfer collision is, therefore, a reduction of the momentum of the ionized solar wind (equal to the momentum of the newly produced neutral atom) and an increase in the solar wind thermal energy (equal to the energy of circular motion of the newly produced proton). We have avoided in this discussion explicit consideration of the effects of finite solar wind temperature and finite flow speed (relative to the Sun) of interstellar neutrals, but both these effects are quite small.

The two principal effects of interstellar neutral hydrogen on the supersonic solar wind are thus a slowing and heating of the flow (Semar 1970, Wallis 1971a,b, 1973, 1974, Holzer 1972). The aspect of the slowing of the flow in which we are particularly interested is the reduction of the solar wind ram pressure through interaction with the interstellar neutrals, and this reduction can be represented by the factor  $\gamma$ , i.e.

$$\gamma = e^{-\tau_p}, \quad 20.$$

$$\tau_p = 3 \times 10^{-3} F_t \left( \frac{n_H}{0.1} \right) (R_s - 5), \quad 21.$$

where the solar wind ram pressure at the terminal shock (upstream in the interstellar wind) is  $\gamma \rho u^2$ , and  $F_t$  is the factor by which the interstellar neutral hydrogen density is decreased from its interstellar value at the terminal shock (cf. Equations 14–16). Away from the direction upstream in the interstellar wind, the hydrogen density inside the terminal shock is a bit lower, so the slowing effect is reduced and  $\gamma$  is correspondingly larger.

Beyond about 5 AU from the Sun, the heating of the supersonic solar wind arising from the interaction with interstellar neutrals is larger than the cooling associated with the spherical expansion of the wind. Thus, one might expect such heating to be observable by spacecraft in the outer solar system. Yet this heating is comparable to that produced by solar wind stream interactions (e.g. Hundhausen 1973, Pizzo 1986, Burlaga 1988)

near the ecliptic plane (which is where the spacecraft are located), so distinguishing between the two heating processes would be difficult under the best of circumstances. A further difficulty, however, is presented by the fact that while the pickup ions rapidly pitch-angle scatter to form a spherical shell in velocity space (at a speed several times the proton thermal speed), they diffuse very slowly in energy and thus do not become assimilated into the ambient near-equilibrium solar wind proton velocity distribution (Isenberg 1987). Thus, instruments designed to observe a highly directed proton velocity distribution (characteristic of a highly supersonic flow) are at a distinct disadvantage in seeking that part of the distribution (the pickup ions) for which the random speed is comparable to the flow speed. Fortunately, there have been observations of singly ionized helium pickup ions (Mobius et al. 1985, Mobius 1986), and these observations seem to confirm the description of pickup ions just given. Although the lack of assimilation of pickup ions into the ambient solar wind velocity distribution is largely irrelevant to the description of solar wind dynamics (e.g. the effect of the solar wind pressure gradient force), it is quite important for particle acceleration at the terminal shock, as is discussed in Section 3.6.2.

**3.5.3 EFFECTS OF NEUTRALS ON THE POSTSHOCK, SUBSONIC SOLAR WIND FLOW** In the region of postshock, subsonic solar wind, where the proton temperature remains high ( $T \gtrsim 10^6$  K), charge transfer between a solar wind proton and an interstellar hydrogen atom produces a fast neutral atom (cf. Section 3.5.1) that is very unlikely to undergo another charge transfer collision until it is well outside the heliosphere. As this atom leaves the heliosphere, it carries with it some of the thermal energy and (on average) the momentum of the subsonic wind, so it follows that the charge transfer collision producing the fast neutral atom serves to cool the subsonic solar wind and to turn its flow into the direction of the interstellar neutral gas flow. In the hemisphere toward the incoming interstellar wind, this turning of the flow is aided by the magnetic force directed from solar equator to pole that arises from the more rapid decline of the magnetic pressure at high latitudes and from the component of the magnetic tension force directed from equator to pole (Parker 1958, 1963).

In order to estimate the distance traveled by the subsonic solar wind before it is turned to flow in the direction of the interstellar wind, we need to consider the time required for the subsonic flow to reach a given radial distance. As mentioned earlier (Section 3.4), in the region where the subsonic flow is nearly incompressible the flow speed decreases as  $r^{-2}$ , so the time (in seconds) taken to travel from the shock radius  $R_s$  to a radius  $R$  is

$$t = 5 \times 10^5 \left( \frac{10^7}{u_s} \right) R_s \left[ \left( \frac{R}{R_s} \right)^3 - 1 \right], \quad 22.$$

where  $u_s$  is the flow speed (centimeters per second) just downstream of the terminal shock. The fraction of solar wind protons that undergo charge transfer with interstellar neutrals during this time  $t$  is just  $(1 - e^{-\tau_p})$ , where

$$\tau_p = 2 \times 10^{-3} \left( \frac{n_H}{0.1} \right) F(R) R_s \left[ \left( \frac{R}{R_s} \right)^3 - 1 \right], \quad 23.$$

and  $F(R)$  is the factor by which the interstellar hydrogen density is reduced at the radius  $R$ . The turning of the flow should be accomplished when  $\tau_p$  reaches a value of about 2, and for a minimum shock distance of  $R_H = 50$  AU, this corresponds to a minimum heliopause distance  $R_H$  that is 2 or 3 times  $R_s$ .

Once the subsonic solar wind flow is turned into the heliospheric tail (cf. Section 3.8 and Figure 5) it rapidly (within several  $R_s$ ) reaches velocity and temperature equilibrium with the neutral interstellar gas. Such an adjustment of the heliosphere to the interstellar medium could not be accomplished without the relatively free penetration of interstellar neutral hydrogen into the heliosphere.

### 3.6 Cosmic-Ray Effects

As noted earlier, Galactic cosmic rays penetrate relatively freely into the heliosphere and thus, like the interstellar neutral gas, can interact directly with both the supersonic and the postshock subsonic solar wind (Section 3.6.1). Yet it appears that the cosmic rays that are most important to our study of the interaction between the solar wind and the interstellar medium are accelerated in the heliosphere itself and comprise ions that were once interstellar neutral atoms that penetrated into the region of supersonic solar wind before being ionized (Section 3.6.2). We now briefly discuss both these interactions.

**3.6.1 GALACTIC COSMIC RAYS** As Galactic cosmic rays flow through the heliosphere, they scatter off magnetic fluctuations transported outward by the solar wind (Parker 1956). Through this scattering the solar wind exerts a radially outward force on the cosmic rays, which is balanced by an inward cosmic-ray pressure gradient force. The cosmic-ray pressure gradient force, of course, affects momentum balance in both the subsonic and the supersonic solar wind and thus affects the location of the terminal shock (e.g. Axford & Newman 1965, Jokipii & Parker 1967, Souk & Lenchek 1969, Wallis 1971a). Recent calculations (Axford & Ip 1986, Ko & Webb 1987, 1988, Ko et al. 1988) indicate that the ram pressure in the supersonic solar

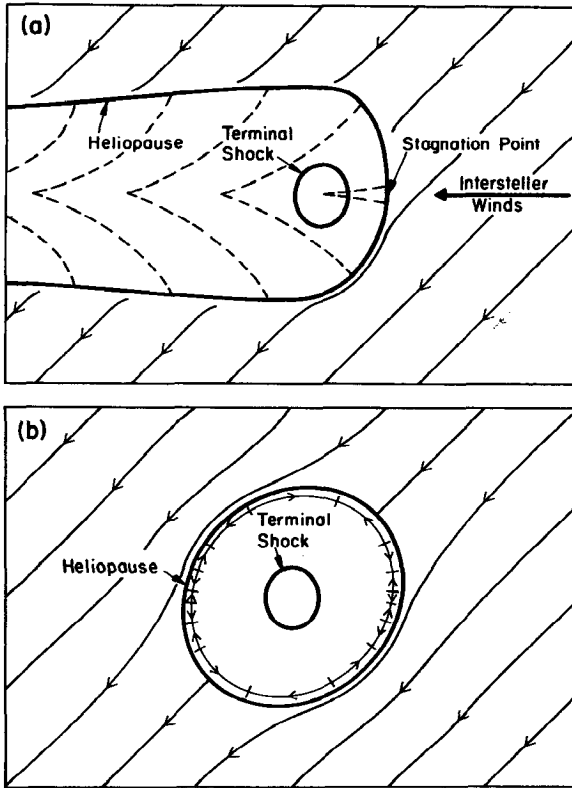


*Figure 5* Schematic illustration of the structure of the heliosphere in a magnetically dominated interstellar medium: (a) plane containing the interstellar velocity vector and the solar rotation axis (assumed normal to  $u_i$ ); (b) plane perpendicular to the interstellar velocity vector and containing the solar rotation axis. Light arrows outside the heliosphere indicate the direction of the component of the interstellar magnetic field in the plane shown. Dashed curves in panel *a* are loci of solar wind fluid elements emitted from the Sun near the solar equator at the maximum of every third 11-yr solar cycle. The arrows paralleling the heliopause in panel *b* indicate the predominant direction of the component (in the plane of the paper) of the heliospheric magnetic field within a few astronomical units of the heliopause. The 16 places where the field changes direction correspond to boundaries between plasma emitted from the Sun during successive 11-yr solar cycles.

wind is reduced by about 5–10% by the cosmic-ray pressure gradient, while the pressure of cosmic rays excluded from the supersonic region is much less than the total cosmic-ray pressure...

**3.6.2 COSMIC-RAY ANOMALOUS COMPONENT:** An anomalous enhancement is observed in the cosmic-ray spectrum at low energies (5–50 MeV

nucleon<sup>-1</sup>) for elements such as He, N, O, and Ne (e.g. Garcia-Munoz et al. 1973, Hovestadt et al. 1973, McDonald et al. 1974, von Rosenwinge & McDonald 1975, Cummings & Stone 1988). It has been suggested (Fisk et al. 1974) that this cosmic-ray anomalous component arises from interstellar neutral atoms that have penetrated into the region of supersonic solar wind, have been ionized, and have been accelerated to MeV energies. A possible mechanism for the last stage of this process is acceleration of the interstellar pickup ions at the solar wind terminal shock (Fisk 1986, Jokipii 1986). The observed increase in the anomalous component with radial distance, together with the assumption that the anomalous component contains hydrogen in appropriate proportion to its other constituents [anomalous hydrogen is presumably masked by Galactic cosmic-ray protons in the inner heliosphere (Beatty et al. 1985)], implies that if the anomalous component is accelerated at the terminal shock, then the shock must be located inside 50 AU in order that the anomalous hydrogen pressure not exceed the solar wind ram pressure upstream of the shock (Fisk 1986, Jokipii 1986, Lee 1988). Of course, if the anomalous hydrogen pressure is relatively large upstream of the terminal shock, then it should significantly modify the structure of the shock (Drury 1988, Lee & Axford 1988), but it will not affect the shock location (e.g. Lee 1988).

### 3.7 *Effect of Interstellar Dust*

The last interstellar component we consider is dust, and we assume that in the VLISM the gas-to-dust mass ratio is 100 and that the typical grain radius is  $5 \times 10^{-6} \lesssim a \lesssim 2 \times 10^{-5}$  cm (e.g. Greenberg 1978). Assuming that in the heliosphere a dust grain is charged to 5 V (e.g. Parker 1964, Lamy et al. 1985), we can readily calculate (Parker 1964) the Lorentz force on the grain ( $G_L$ ), which is the same force exerted on interstellar pickup ions by the magnetized solar wind, and compare it with the solar gravitational and radiative forces exerted on the grain ( $G_G$  and  $G_R$ ):

$$G_L \approx 1.5 \times 10^{-10} \left( \frac{u_E}{10^7} \right) \frac{a}{R} \text{ dyn}, \quad 24.$$

$$G_G \approx 7 \frac{a^3}{R^2} \text{ dyn}, \quad 25.$$

$$G_R \approx 1.4 \times 10^{-4} \frac{a^2}{R^2} \text{ dyn}, \quad 26.$$

where  $a$  is the grain radius,  $R$  is the heliocentric radial distance, and  $u_E$  is the solar wind flow speed at 1 AU. For  $a = 10^{-5}$  cm,  $R = 100$  AU, and  $u_E = 5 \times 10^7$  cm s<sup>-1</sup>, the Lorentz force is 100 times the gravitational force

and 50 times the radiative force, so it is clear that such dust grains will be excluded from the heliosphere (e.g. Levy & Jokipii 1976). Interstellar dust, therefore, will exert a surface force at the heliopause, but this force is negligible in comparison with the other interstellar forces we are considering.

### 3.8 Structure of the Heliosphere

We have now provided an adequate observational and theoretical basis for discussing the expected large-scale structure of the heliosphere. A schematic view of this structure for a magnetically dominated VLISM<sup>1</sup> is given in Figure 5, where two cross sections of the heliosphere are shown: (a) the plane containing both the interstellar velocity vector (in the solar rest frame) and the solar rotation axis; and (b) the plane perpendicular to the interstellar velocity vector and containing the solar rotation axis. For convenience, the solar rotation axis is taken to be perpendicular to the interstellar wind vector, although the angle between the two vectors actually may be closer to 97° (cf. Section 2.2.1). If the VLISM is dominated by thermal gas pressure rather than magnetic pressure (which we consider unlikely), some aspects of the heliosphere and VLISM illustrated in Figure 2 must be taken into account. Thus, with attention directed to Figures 5 and 2, we proceed with a consideration of heliospheric structure, concentrating on the locations and shapes of the terminal shock (which bounds the region of supersonic solar wind flow) and of the heliopause (which bounds the region of influence of the solar magnetized plasma).

**3.8.1 THE TERMINAL SHOCK** As in Section 3.1, we first determine the shock distance along the stagnation line (cf. Figure 2),  $R_s$ , by equating the total pressures just inside and just outside the heliopause at the stagnation point (cf. Figure 5):

$$\gamma_1 \gamma_2 \gamma_3 \rho_E u_E^2 / R_s^2 = \Gamma_1 B_1^2 / 8\pi + (2n_c + \Gamma_2 n_H) (\Gamma_3 k T_1 + \Gamma_4 m_H u_1^2) + \Gamma_5 p_{cr} + \Gamma_6 \rho_d u_1^2 \quad 27.$$

The total pressure just inside the heliopause, which is given by the left side of Equation 27, is written in terms of the solar wind ram pressure at 1 AU

<sup>1</sup>Note that when we speak of a magnetically dominated VLISM in the context of heliospheric structure, we are not addressing the issue of the relative energy densities of magnetic field and fluid (thermal gas and cosmic rays) in the interstellar medium. Consider, for example, the case of a 5- $\mu$ G magnetic field and a negligible thermal gas pressure. The magnetic pressure is  $10^{-12}$  dyn  $\text{cm}^{-2}$ , which is about the same as the Galactic cosmic-ray pressure. Yet the magnetic field is enhanced near the heliosphere by up to a factor of 4, while only a small fraction of the cosmic-ray pressure plays a role in determining the structure of the heliosphere. Thus, from the standpoint of heliospheric structure, the VLISM is magnetically dominated despite the near equipartition of energy between field and fluid.

( $\rho_E u_E^2$ ), the factors by which the ram pressure is reduced between 1 AU and the terminal shock through spherical expansion ( $R_s^{-2}$ , where  $R_s$  is in astronomical units) and through interaction with the interstellar neutral gas ( $\gamma_1$ ) and Galactic cosmic rays ( $\gamma_2$ ), and the factor by which the total pressure at the heliopause is reduced from the ram pressure just inside the terminal shock ( $\gamma_3$ ). The total pressure just outside the heliopause, which is given by the right side of Equation 27, is separated into four terms, associated with the interstellar magnetic field, the interstellar thermal gas (neutral and ionized components), Galactic cosmic rays, and interstellar dust. The factor  $\Gamma_1$  reflects the amplification of the background interstellar magnetic field through distortion by the heliosphere (cf. Section 3.3, and Figures 3 and 4). The factors  $\Gamma_2$  and  $\Gamma_5$  are, respectively, the fractions of interstellar neutrals and of Galactic cosmic rays (i.e. cosmic-ray pressure) excluded from the supersonic solar wind. (Note that for simplicity we are treating this exclusion in Equation 27 like an exclusion from the heliosphere.) Finally, the factors  $\Gamma_3$ ,  $\Gamma_4$ , and  $\Gamma_6$  are all of order 1 and reflect the nature of the flow around the heliosphere; illustrative values of  $\Gamma_3$  and  $\Gamma_4$  for the two types of flow shown in Figure 2 are given by Equations 9 and 10.

In the discussion of Sections 2 and 3 we have given ranges of possible values for the various parameters that determine the terminal shock distance in Equation 27. We first calculate the shock distances for both low-speed and high-speed solar wind (cf. Table 1) appropriate to the midpoints of these parameter ranges, and then we perform the calculations for extreme values of the parameters in order to produce minimum and maximum values for the shock distance. For the first calculation (using midpoints of the parameter ranges), we take  $\gamma_1 = 0.89$ ,  $\gamma_2 = 0.93$ , and  $\gamma_3 = 0.5$ . The value of  $\gamma_3$  (cf. Section 3.4) is determined using the results of Holzer (1972) and by assuming a heliopause distance that is between 2 and 3 times the shock distance along the stagnation line. A value of  $\Gamma_1 = 2.5$  is determined by assuming that the interstellar magnetic field is oriented at  $45^\circ$  to the interstellar wind vector and that a maximum amplification factor<sup>2</sup> of  $\Gamma_1 = 4$  is appropriate for an orientation of  $90^\circ$ . [Compare this with the value of  $\Gamma_1 = 2.25$  (cf. Section 3.3) normally assumed (e.g. Axford 1972, Axford & Ip 1986, Lee 1988).] For the remaining factors, we choose  $\Gamma_5 = 0.23$  (cf. Section 2.2.4),  $\Gamma_2 = 1 - F_t = 0.1$  (cf. Section 3.5.1), and  $\Gamma_3 = \Gamma_4 = \Gamma_6 = 1$ . It follows that the shock distances (for low-speed and high-speed solar wind) appropriate to the midpoints of the parameter ranges are

<sup>2</sup>We use the amplification factor appropriate to the cylinder in Figure 3b, because the heliospheric tail is presumably nearly cylindrical, and all flow lines leaving the terminal shock must have an asymptotic pressure corresponding to that of the heliospheric tail.

$$R_s(\text{low speed}) = 50 \text{ AU}, \quad 28.$$

$$R_s(\text{high speed}) = 60 \text{ AU}. \quad 29.$$

Taking extreme values of the parameters, we obtain the following maximum and minimum values for the shock distance, again for both low-speed and high-speed wind:

$$R_{s \text{ min}}(\text{low speed}) = 25 \text{ AU}, \quad 30.$$

$$R_{s \text{ max}}(\text{low speed}) = 140 \text{ AU}, \quad 31.$$

$$R_{s \text{ min}}(\text{high speed}) = 27 \text{ AU}, \quad 32.$$

$$R_{s \text{ max}}(\text{high speed}) = 170 \text{ AU}. \quad 33.$$

An examination of the relative magnitudes of the terms on the right side of Equation 27 reveals that the principal source of uncertainty in the terminal shock location (as reflected in Equations 30–33) is the uncertainty in the interstellar magnetic field. It follows that a direct detection of the shock would indirectly place a significant constraint on the magnetic field of the VLISM and would thus make an important contribution to our understanding of the ISM. (We note, however, that for the very low value of  $B_1 \approx 2 \times 10^{-6}$  G used in calculating  $R_{s \text{ max}}$ , the reduction of  $\gamma_1$  through slowing of the supersonic wind by interstellar neutral hydrogen quite significantly reduces  $R_{s \text{ max}}$ .)

The different shock distances for low-speed and high-speed wind indicate that the terminal shock is not likely to be spherical; rather, it should bulge outward at high solar latitudes, where high-speed wind flows over most of the solar cycle (cf. Section 2.1). The shortest distance to the terminal shock should be along the stagnation line, where the lowest speed wind usually flows and where the modest effect of the interstellar ram pressure is felt most strongly; the antipodal shock distance, however, should only be slightly greater than this shortest distance. Although the distortion in shape of the terminal shock is modest, the density difference at high and low latitudes is large, with the high-latitude (high-speed wind) shock density being about a factor of 4 less than the low-latitude (low-speed wind) shock density. Of course, during the declining phase of the solar cycle, when a mixture of high-speed and low-speed wind flows within some  $30^\circ$  of the solar equator (e.g. Hundhausen 1977), the density ratio will be somewhat less (something like 2.5 to 3). This substantial density difference at low and high latitudes could lead to two spectral peaks in radio emission from the terminal shock and thus might be consistent with the observations of Kurth et al. (1984, 1987; cf. Section 2.3).

The preceding discussion has not touched upon shock motion in

response to variations of the solar wind on time scales ranging from 25 days [shorter time-scale variations are filtered out in the inner heliosphere (e.g. Pizzo 1986)] to 11 yr (period of the solar activity cycle). The detailed adjustment of the terminal shock to such variations will generally be relatively complex, often involving the formation and eventual dissipation of multiple shocks (including both forward and reverse shocks). On average, though, the terminal shock should move about 2–3 AU a month in response to solar wind ram pressure changes, so only the relatively long-period solar wind variations should produce a significant change in the shock location. Of course, even quite small changes in the shock location will lead to multiple shock crossings by a spacecraft, and such multiple crossings will have to be carefully distinguished from the crossing of multiple shocks mentioned above.

**3.8.2 THE HELIOPAUSE** The basic shape of the heliopause is determined by the turning of the subsonic solar wind flow and by the containment of the heliospheric magnetized plasma with the pressure of the interstellar magnetized plasma. The turning of the flow is accomplished in part through the frictionlike interaction between interstellar neutral hydrogen atoms and solar wind protons, in part through the asymmetry of the terminal shock (which turns the flow poleward), and in part through the poleward Lorentz force, which becomes important as the heliospheric magnetic field becomes dominant [well beyond the terminal shock (cf. Section 3.4)]. The interstellar neutrals not only play a major role in turning the postshock solar wind flow, but they also bring the heliospheric plasma toward both flow and temperature equilibrium with the interstellar gas just a few  $R_s$  into the heliospheric tail. The evolution toward temperature equilibrium, of course, brings about a modest compression of the heliospheric plasma in the tail, which accounts for the slight narrowing of the heliosphere downstream in the interstellar wind shown in Figure 5.

The distortion of the heliopause by the inherent anisotropy of the interstellar magnetic stress on the heliosphere is shown in Figure 5 (especially panel *b*) as being much more modest than one might expect from Figure 4. This reduction in distortion results from the substantial component of the interstellar field parallel to the axis of the heliospheric tail [ $(\mathbf{B}_1 \cdot \mathbf{u}_1)^2 / (B_1^2 u_1^2) = 0.5$  in Figure 5], which contrasts with the absence of a magnetic field component parallel to the axis of the cylinder in Figure 4. Such a parallel field component in Figure 3*b* would lead to a change in magnetic field pressure along  $r = a$  (from  $\theta = 90^\circ$  to  $\theta = 0^\circ$ ) from 2.5 to 0.5 times the background pressure, rather than from 4 to 0 times the background pressure. Evidently, the component of the interstellar field parallel to the axis of the heliospheric tail also leads to a reduction of

the amplification of the interstellar field caused by the presence of the heliosphere (cf. Section 3.3), which we accounted for when assigning a value to  $\Gamma_1$  in Section 3.8.1.

One might expect (e.g. Fahr et al. 1986) substantial diffusion across the heliopause, rapidly obscuring completely the boundary between the heliosphere and the VLISM. However, in the magnetically dominated model shown schematically in Figure 5, such diffusion should be quite small. Generation of the Kelvin-Helmholtz instability is suppressed because of the rapid approach to flow equilibrium across the heliopause induced by the interstellar neutrals. Furthermore, magnetic field line reconnection should not be particularly significant for the following reasons.

First, let us consider the predominant direction of the heliospheric magnetic field within several astronomical units of the heliopause. We begin by noting that loci of solar wind fluid elements emitted from the Sun near the solar equator at the maximum of every third 11-yr solar cycle are shown in projection by the dashed curves in Figure 5*a*. The direction of the solar magnetic field reverses (at solar maximum) from one solar cycle to the next, in the sense that in one solar cycle the field is directed predominantly outward from the Sun in the Northern Hemisphere and predominantly inward toward the Sun in the Southern Hemisphere, while in the preceding and following cycles these directions are reversed. Because the solar rotation axis is nearly perpendicular to the interstellar wind vector and because the heliospheric field is wrapped into a tight spiral (cf. Section 3.4), the component of the predominant heliospheric field in a plane perpendicular to the axis of the heliospheric tail (like that shown in Figure 5*b*) will be counterclockwise (in both hemispheres) in one solar cycle and clockwise in the preceding and following cycles. Thus, since postshock solar wind originating from the Sun during part or all of five solar cycles appears in the plane of Figure 5*b* (cf. dashed loci in Figure 5*a*), there are 16 reversals (of the component in the plane of Figure 5*b*) of the predominant field direction in the vicinity of the heliopause. [Actually, there will be many more field reversals because of the tilt and distortion of the neutral sheet separating the oppositely directed solar fields in the Northern and Southern Hemispheres (e.g. Hundhausen 1977), but the 16 reversals shown in Figure 5*b* adequately illustrate our point.] Reconnection can take place at a reasonably rapid rate only when the components of the interstellar and heliospheric fields shown in Figure 5*a* are oppositely directed, and any reconnection that does take place will eventually lead to the replacement of the reconnected heliospheric field with oppositely directed field from an adjacent heliospheric region. Thus, a skin of heliospheric magnetic field with a direction inappropriate to reconnection with

the interstellar field will form at the heliopause, and the reconnection process will be suppressed.

In the absence of significant reconnection or disruption by the Kelvin-Helmholtz instability, it seems likely that the heliopause shown in Figure 5 will maintain its integrity far into the heliospheric tail. Of course, there will be reconnection at current sheets within the heliospheric tail, but this is not likely to affect the heliopause significantly and, indeed, should not be able to maintain the mean heliospheric tail temperature significantly above the interstellar gas temperature.

#### 4. CONCLUDING REMARKS

Given the observational and theoretical information currently available, it appears that the interaction between the solar wind and the VLISM is characterized primarily by the interstellar magnetic containment of the solar magnetized plasma and by the slowing, turning, and cooling of the postshock subsonic solar wind flow through charge transfer with interstellar H atoms. The shock terminating supersonic solar wind flow (and thus accommodating the flow to the interstellar pressure) should be asymmetric, with the greatest shock distance at high latitudes, where the predominantly high-speed solar wind is characterized by a larger ram pressure than the lower speed wind flowing near the solar equator.

The distance to the solar wind terminal shock is very sensitive to the magnitude (and, to a lesser extent, to the direction) of the VLISM magnetic field. Recent indirect inferences of a shock distance of 50 AU (or a bit less) are not inconsistent with current observational estimates of this field, but unfortunately the same could be said of inferences of a shock distance of some 150 AU. If the terminal shock does lie near 50 AU, then the *Voyager 1* spacecraft should cross it within the next few years, and such a crossing would obviously place an important constraint on the interstellar magnetic field.

Clearly, the most important information to acquire in furthering our understanding of the interaction between the solar wind and the VLISM is a considerably improved determination of the VLISM magnetic field, but this is not likely to be obtainable in the near future. It is, therefore, imperative to maintain operation as long as possible of all our deep space missions, in the not-unreasonable hope that we can either directly or indirectly determine the location of the solar wind terminal shock. The observations most likely to be helpful in such a determination are of the plasma, magnetic field, plasma waves, and energetic particles, but it is also important to continue studying the UV radiation scattered by interstellar neutrals that have penetrated into the heliosphere. These UV observations, obtained both from deep space probes and from spacecraft in the inner

heliosphere, can provide us not only with information concerning the VLISM ionization state (although only if the observational uncertainties are reduced), but also with valuable information concerning the latitudinal variation of the solar wind mass flux, which is important to our understanding of solar wind acceleration near the Sun (e.g. Lallement et al. 1986).

An obvious lesson to be learned from consideration of the interaction between the solar wind and the interstellar medium is that the community of scientists studying the local interstellar medium and the community of scientists studying the heliosphere should maintain the close contact that has recently been established.

#### ACKNOWLEDGMENTS

I am particularly grateful to B. C. Low for his comments and criticisms on the manuscript, which have led to a significantly improved review (especially Section 3.3). I also wish to thank Randy Jokipii and Marty Lee for useful discussions, and Liz Boyd for preparing the manuscript. This work was supported in part by NASA Contract W-17,016.

#### Literature Cited

- Ajello, J. M. 1978. *Ap. J.* 222: 1068  
Ajello, J. M., Stewart, A. I., Thomas, G. E., Graps, A. 1987. *Ap. J.* 317: 964  
Axford, W. I. 1972. In *Solar Wind*, ed. C. P. Sonett, P. J. Coleman Jr., J. M. Wilcox, p. 609. *NASA SP-308*  
Axford, W. I. 1973. *Space Sci. Rev.* 14: 582  
Axford, W. I. 1976. In *Physics of Solar Planetary Environments*, 1: 270. Washington, DC: Am. Geophys. Union  
Axford, W. I., Dessler, A. J., Gottlieb, B. 1963. *Ap. J.* 137: 1268  
Axford, W. I., Ip, W.-H. 1986. *Adv. Space Res.* 6(2): 27  
Axford, W. I., Newman, R. C. 1965. *Proc. Int. Conf. Cosmic Rays, 9th, London*, p. 173. London: Phys. Soc.  
Baranov, V. B., Krasnobaev, K. V., Kulikovskiy, A. G. 1970. *Dokl. Acad. Sci. USSR* 194: 41  
Baranov, V. B., Krasnobaev, K. V., Ruderman, M. S. 1976. *Astrophys. Space Sci.* 41: 481  
Beatty, J. J., Garcia-Munoz, M., Simpson, J. A. 1985. *Ap. J.* 294: 455  
Bertaux, J. L., Blamont, J. E. 1971. *Astron. Astrophys.* 11: 200  
Bertaux, J. L., Blamont, J. E., Mironova, E. N., Kurt, V. G., Bourgin, M. C. 1977. *Nature* 270: 156  
Bertaux, J. L., Lallement, R., Kurt, V. G., Mironova, E. N. 1985. *Astron. Astrophys.* 150: 1  
Blum, P. W., Fahr, H. J. 1970. *Astron. Astrophys.* 4: 280  
Blum, P. W., Grzedzielski, S., Witt, N. 1980. *Astrophys. Space Sci.* 70: 513  
Brown, R. L., Chang, C.-A. 1983. *Ap. J.* 264: 134  
Burlaga, L. F. 1988. *Proc. Int. Sol. Wind Conf., 6th*, ed. V. J. Pizzo, T. E. Holzer, D. G. Sime, p. 547. *NCAR/TN-306 + Proc Chassefiere, E., Bertaux, J. L. 1987a. Astron. Astrophys.* 174: 239  
Chassefiere, E., Bertaux, J. L. 1987b. *Astron. Astrophys.* 176: 121  
Chassefiere, E., Bertaux, J. L., Lallement, R., Kurt, V. G. 1986. *Astron. Astrophys.* 160: 229  
Chassefiere, E., Bertaux, J. L., Lallement, R., Sandel, B. R., Broadfoot, L. 1988a. *Astron. Astrophys.* 199: 304  
Chassefiere, E., Dalaudier, F., Bertaux, J. L. 1988b. *Astron. Astrophys.* 201: 113  
Clauser, F. 1960. *Symp. Cosmical Gas Dyn., 4th, Varenna, Italy*, p. 306. Bologna: Nicola Zanichelli  
Cox, D. P., Reynolds, R. J. 1987. *Annu. Rev. Astron. Astrophys.* 25: 303  
Cranfill, C. 1971. PhD dissertation. Univ. Calif., San Diego  
Cummings, A. C., Stone, E. C. 1988. *Proc.*

- Int. Sol. Wind Conf.*, 6th, ed. V. J. Pizzo, T. E. Holzer, D. G. Sime, p. 599. *NCAR/TN-306 + Proc*
- Dalaudier, F., Bertaux, J. L., Kurt, V. G., Mironova, E. N. 1984. *Astron. Astrophys.* 134: 171
- Davis, L. Jr. 1955. *Phys. Rev.* 100: 1440
- Davis, L. Jr. 1962. *J. Phys. Soc. Jpn.* 17A-II: 543
- Drury, L. O. 1988. *Proc. Int. Sol. Wind Conf.*, 6th, ed. V. J. Pizzo, T. E. Holzer, D. G. Sime, p. 521. *NCAR/TN-306 + Proc*
- Fahr, H. J. 1974. *Space Sci. Rev.* 15: 483
- Fahr, H. J., Nass, H. U., Rucinski, D. 1985. *Astron. Astrophys.* 142: 476
- Fahr, H. J., Neutsch, W., Grzedzielski, S., Macek, W., Ratkiewicz-Landowska, R. 1986. *Space Sci. Rev.* 43: 329
- Feldman, W. C., Asbridge, J. R., Bame, S. J., Gosling, J. T. 1977. In *The Solar Output and Its Variations*, ed. O. R. White, p. 351. Boulder: Colo. Assoc. Univ. Press
- Fisk, L. A. 1986. In *The Sun and the Heliosphere in Three Dimensions*, ed. R. G. Marsden, p. 401. Dordrecht: Reidel
- Fisk, L. A., Kozlovsky, B., Ramaty, R. 1974. *Ap. J. Lett.* 190: L35
- Frisch, P. C. 1986. *Adv. Space Res.* 6(1): 345
- Frisch, P. C., York, D. C., Fowler, J. R. 1987. *Ap. J.* 320: 842
- Garcia-Munoz, M., Mason, G. M., Simpson, J. A. 1973. *Ap. J. Lett.* 182: L81
- Greenberg, J. M. 1978. In *Cosmic Dust*, ed. J. A. M. McDonnell, p. 187. New York: Wiley
- Heiles, C. 1976. *Annu. Rev. Astron. Astrophys.* 14: 1
- Holzer, T. E. 1972. *J. Geophys. Res.* 77: 5407
- Holzer, T. E. 1977. *Rev. Geophys. Space Phys.* 15: 467
- Holzer, T. E., Axford, W. I. 1971. *J. Geophys. Res.* 76: 6965
- Hovestadt, D., Voilmer, O., Gloeckler, G., Fan, C. Y. 1973. *Phys. Rev. Lett.* 31: 650
- Hundhausen, A. J. 1968. *Planet. Space Sci.* 16: 783
- Hundhausen, A. J. 1973. *J. Geophys. Res.* 78: 1528
- Hundhausen, A. J. 1977. In *Coronal Holes and High Speed Wind Streams*, ed. J. B. Zirker, p. 225. Boulder: Colo. Assoc. Univ. Press
- Hundhausen, A. J., Hansen, R. T., Hansen, S. F. 1981. *J. Geophys. Res.* 86: 2079
- Ip, W.-H., Axford, W. I. 1985. *Astron. Astrophys.* 149: 7
- Isenberg, P. A. 1987. *J. Geophys. Res.* 92: 1067
- Jokipii, J. R. 1986. *J. Geophys. Res.* 91: 2929
- Jokipii, J. R., Parker, E. N. 1967. *Planet. Space Sci.* 15: 1375
- Ko, C. M., Jokipii, J. R., Webb, G. M. 1988. *Ap. J.* 326: 761
- Ko, C. M., Webb, G. M. 1987. *Ap. J.* 323: 657
- Ko, C. M., Webb, G. M. 1988. *Ap. J.* 325: 296
- Kojima, M., Kakinuma, T. 1987. *J. Geophys. Res.* 92: 7269
- Kurth, W. S. 1988. *Proc. Int. Sol. Wind Conf.*, 6th, ed. V. J. Pizzo, T. E. Holzer, D. G. Sime, p. 667. *NCAR/TN-306 + Proc*
- Kurth, W. S., Gurnett, D. A., Scarf, F. L., Poynter, R. L. 1984. *Nature* 312: 27
- Kurth, W. S., Gurnett, D. A., Scarf, F. L., Poynter, R. L. 1987. *Geophys. Res. Lett.* 14: 49
- Lallement, R., Bertaux, J. L., Kurt, V. G. 1985. *J. Geophys. Res.* 90: 1413
- Lallement, R., Holzer, T. E., Munro, R. H. 1986. *J. Geophys. Res.* 91: 6751
- Lamy, P. L., Lefevre, J., Millet, J., Lafon, J. P. 1985. In *Properties and Interactions of Interplanetary Dust*, ed. R. H. Giese, P. Lamy, p. 335. Dordrecht: Reidel
- Lazarus, A., Belcher, J. 1988. *Proc. Int. Sol. Wind Conf.*, 6th, ed. V. J. Pizzo, T. E. Holzer, D. G. Sime, p. 533. *NCAR/TN-306 + Proc*
- Lee, M. A. 1988. *Proc. Int. Sol. Wind Conf.*, 6th, ed. V. J. Pizzo, T. E. Holzer, D. G. Sime, p. 635. *NCAR/TN-306 + Proc*
- Lee, M. A., Axford, W. I. 1988. *Astron. Astrophys.* 194: 297
- Levy, E. H., Jokipii, J. R. 1976. *Nature* 264: 424
- McDonald, F. B., Teegarden, B. J., Trainor, J. H., Webber, W. R. 1974. *Ap. J. Lett.* 187: L105
- McKee, C. F., Ostriker, J. P. 1977. *Ap. J.* 218: 148
- McNutt, R. L. Jr. 1988. *Geophys. Res. Lett.* 15: 1307
- Meier, R. R. 1980. *Astron. Astrophys.* 91: 62
- Mobius, E. 1986. *Adv. Space Res.* 6(1): 199
- Mobius, E., Hovestadt, D., Klecker, B., Scholer, M., Gloeckler, G., Ipavich, F. M. 1985. *Nature* 318: 426
- Paresce, F., Bowyer, S. 1973. *Astron. Astrophys.* 27: 399
- Parker, E. N. 1956. *Phys. Rev.* 103: 1518
- Parker, E. N. 1958. *Ap. J.* 128: 664
- Parker, E. N. 1961. *Ap. J.* 134: 20
- Parker, E. N. 1963. *Interplanetary Dynamical Processes*. New York: Interscience
- Parker, E. N. 1964. *Ap. J.* 139: 951
- Patterson, T. N. L., Johnson, F. S., Hanson, W. B. 1963. *Planet. Space Sci.* 11: 767
- Pesses, M. E., Jokipii, J. R., Eichler, D. 1981. *Ap. J. Lett.* 246: L85
- Pizzo, V. J. 1986. *Adv. Space Res.* 6(1): 353
- Ripken, H. W., Fahr, H. J. 1983. *Astron. Astrophys.* 122: 181
- Schwenn, R. 1983. In *Solar Wind Five*, ed. M. Neugebauer, p. 489. Washington, DC: NASA

- Semar, C. L. 1970. *J. Geophys. Res.* 75: 6892
- Sime, D. G. 1983. In *Solar Wind Five*, ed. M. Neugebauer, p. 453. Washington, DC: NASA
- Sousk, S. F., Lenchek, A. M. 1969. *Ap. J.* 158: 781
- Steinitz, R., Eyni, M. 1980. *Ap. J.* 241: 417
- Suess, S. T., Dessler, A. J. 1985. *Nature* 317: 702
- Tawara, H., Kato, T., Nakai, Y. 1983. *Rep. IPPJ-AM-30*, Inst. of Plasma Phys., Nagoya Univ., Jpn.
- Thomas, G. E. 1978. *Annu. Rev. Earth Planet. Sci.* 6: 173
- Thomas, G. E., Krassa, R. F. 1971. *Astron. Astrophys.* 11: 218
- Thompson, R. C., Nelson, A. H. 1980. *MNRAS* 191: 863
- Tinsley, B. A. 1971. *Rev. Geophys. Space Phys.* 9: 89
- Torland, T. H., Heiles, C. 1986. *Ap. J.* 301: 339
- Vidal-Madjar, A. 1977. In *The Solar Output and Its Variations*, ed. O. R. White, p. 213. Boulder: Colo. Assoc. Univ. Press
- von Rosenwinge, T. T., McDonald, F. B. 1975. *Proc. Int. Cosmic Ray Conf., 14th, Munich*, 2: 792
- Wallis, M. 1971a. *Rep. TRITA-EPP-71-01*, R. Inst. Technol., Stockholm, Swed.
- Wallis, M. 1971b. *Nature* 233: 23
- Wallis, M. K. 1973. *Astrophys. Space Sci.* 20: 3
- Wallis, M. 1974. *MNRAS* 167: 103
- Wallis, M. K. 1975. *Nature* 254: 202
- Wallis, M. K. 1978. *Space Res.* 18: 401
- Wallis, M. K. 1981. In *Solar Wind Four*, ed. H. Rosenbauer, p. 516. Katlenburg-Lindau, Germ: MPAE
- Wallis, M. K. 1984. *Astron. Astrophys.* 130: 200
- Wallis, M. K. 1988. *Proc. Int. Sol. Wind Conf., 6th*, ed. V. J. Pizzo, T. E. Holzer, D. G. Sime, p. 687. *NCAR/TN-306+ Proc*
- Wallis, M. K., Hassan, M. H. A. 1978. *Planet. Space Sci.* 26: 111
- Wallis, M. K., Wallis, J. 1979. *Astron. Astrophys.* 78: 41
- Webber, W. R. 1987. *Astron. Astrophys.* 179: 277
- Weller, C. S., Meier, R. R. 1981. *Ap. J.* 246: 386
- Weymann, R. 1960. *Ap. J.* 132: 390
- Wu, F. M., Gangopadhyay, P., Ogawa, H. S., Judge, D. L. 1988. *Ap. J.* 331: 1004



## CONTENTS

DREAMS, STARS, AND ELECTRONS, <i>Lyman Spitzer, Jr.</i>	1
THE STATUS AND PROSPECTS FOR GROUND-BASED OBSERVATORY SITES, <i>R. H. Garstang</i>	19
THE ORION MOLECULAR CLOUD AND STAR-FORMING REGION, <i>Reinhard Genzel and Jürgen Stutzki</i>	41
X RAYS FROM NORMAL GALAXIES, <i>G. Fabbiano</i>	87
POPULATIONS IN LOCAL GROUP GALAXIES, <i>Paul Hodge</i>	139
A NEW COMPONENT OF THE INTERSTELLAR MATTER: Small Grains and Large Aromatic Molecules, <i>J. L. Puget and A. Léger</i>	161
INTERACTION BETWEEN THE SOLAR WIND AND THE INTERSTELLAR MEDIUM, <i>Thomas E. Holzer</i>	199
SURFACE PHOTOMETRY AND THE STRUCTURE OF ELLIPTICAL GALAXIES, <i>John Kormendy and S. Djorgovski</i>	235
ABUNDANCE RATIOS AS A FUNCTION OF METALLICITY, <i>J. Craig Wheeler, Christopher Sneden, and James W. Truran, Jr.</i>	279
T TAURI STARS: WILD AS DUST, <i>Claude Bertout</i>	351
ASTROPHYSICAL CONTRIBUTIONS OF THE INTERNATIONAL ULTRAVIOLET EXPLORER, <i>Yoji Kondo, Albert Boggess, and Stephen P. Maran</i>	397
CLASSIFICATION OF SOLAR FLARES, <i>T. Bai and P. A. Sturrock</i>	421
DIFFUSE GALACTIC GAMMA-RAY EMISSION, <i>Hans Bloemen</i>	469
QUASI-PERIODIC OSCILLATIONS AND NOISE IN LOW-MASS X-RAY BINARIES, <i>M. van der Klis</i>	517
KINEMATICS, CHEMISTRY, AND STRUCTURE OF THE GALAXY, <i>Gerard Gilmore, Rosemary F. G. Wyse, and Konrad Kuijken</i>	555
SUPERNOVA 1987A, <i>W. David Arnett, John N. Bahcall, Robert P. Kirshner, and Stanford E. Woosley</i>	629
CHEMICAL ANALYSES OF COOL STARS, <i>Bengt Gustafsson</i>	701
INDEXES	
Subject Index	757
Cumulative Index of Contributing Authors, Volumes 17–27	766
Cumulative Index of Chapter Titles, Volumes 17–27	768